

Electron-phonon energy relaxation in quasi-one-dimensional electron systems in zero and quantizing magnetic fields

A. Y. Shik

A. F. Ioffe Physical-Technical Institute, 194021 St. Petersburg, Russia

L. J. Challis

Department of Physics, University of Nottingham, NG7 2RD, United Kingdom

(Received 26 May 1992; revised manuscript received 21 August 1992)

The nature of the acoustic-phonon emission from a quasi-one-dimensional electron gas has been shown to vary with electron temperature T_e and confinement potential. Intensity oscillations occur as the one-dimensional levels are moved through the Fermi level E_F and quasimonochromatic phonons are emitted at higher temperatures. Analytical expressions have been obtained for the frequency spectrum of the total energy-loss rate Q and very marked changes with T_e are predicted in the angular distribution of emitted phonons. The emission is strongly affected by magnetic field. At low T_e , oscillatory behavior of Q at relatively low field is replaced by a monotonic increase followed by a sharp fall when the Fermi velocity drops below the velocity of sound. Marked changes should also occur in the angular distribution.

I. INTRODUCTION

The main task of this paper is to calculate the electron energy relaxation due to acoustic-phonon emission from a (quasi-)one-dimensional electron gas (1DEG) in both zero and quantizing magnetic fields B . A number of calculations have now been made of phonon emission from 2DEG's (Refs. 1–5, $B=0$ —these references refer to GaAs and Refs. 6 and 7, $B \neq 0$) and there has also been a substantial amount of experimental investigation. The experiments include direct measurements of the angular and frequency distributions of emitted phonons $W(\mathbf{q})$ (Refs. 8 and 9) and also studies of the integral energy-loss rate Q .^{3,10,11} However no experimental studies of emission from 1DEG's have been reported yet and there has only been one theoretical treatment.¹² This paper, which also included analysis of phonon emission from quantum dots, concentrated on the numerical calculations of the integral energy-loss rate. Little detailed information was given on the angular and frequency distribution and the analysis was confined to zero magnetic fields.

In the present work we give particular attention to the form of $W(\mathbf{q})$ for the different ranges of parameters and also consider the effects of quantizing magnetic fields. An outline of these results has been given in a preliminary communication.¹³ The analysis has applications which extend beyond ultrathin wires or electrostatically confined structures. Important examples are the one-dimensional edge states that exist on either side of a Hall bar when a quantizing magnetic field is applied; many of the properties of the quantum Hall effect can be described in terms of quasi-one-dimensional edge currents passing through these states.¹⁴ The confinement is now due to both electrostatic and magnetic potentials but, as we shall show in a later paper, the phonon emission can be described in a similar way to that in electrostatically confined systems.

II. THE BASIC EQUATIONS

We consider emission from a 1DEG formed by the lateral confinement of a two-dimensional electron system in the plane $z=0$. We assume the confining potential to be parabolic: $V=m\omega^2x^2/2$ and note that this form has been shown to provide a good description of the behavior of several types of 1D structure.^{15–17} The electron eigenstates and energy eigenvalues of the system are given by

$$\langle N, k | \equiv \psi(x, y) = u_N(x) \exp(iky), \quad (1a)$$

and

$$\epsilon = \hbar\omega(N + \frac{1}{2}) + \hbar^2k^2/2m, \quad (1b)$$

where $u_N(x)$ is a harmonic oscillator function with characteristic width $l=(\hbar/m\omega)^{1/2}$, k is the wave vector in the direction of free motion (y axis), and $N=0, 1, 2, \dots$. We assume that the electron distribution in the 1DEG will be described by a degenerate Fermi function f_e for which the effective electron temperature T_e is greater than the lattice temperature T . If the Fermi energy $E_F < \frac{3}{2}\hbar\omega$ so that only one subband is occupied at low temperatures, E_F increases with linear electron density ν as

$$E_F = \frac{\hbar\omega}{2} + \frac{\pi^2\nu^2\hbar^2}{8m}. \quad (2a)$$

However if $E_F \gg \hbar\omega$ so that many subbands are occupied,

$$E_F = \left[\frac{9\pi^2\hbar^4\omega^2\nu^2}{32m} \right]^{1/3}. \quad (2b)$$

In terms of ν the conditions for these two cases are $\nu < 2\sqrt{2}/\pi l$ and $\nu \gg l^{-1}$, respectively, corresponding to confinement lengths less and greater than the average

electron separation.

For an electronic system with spherical energy surfaces, as in GaAs, the electron acoustic-phonon interaction is described by the potential $V_q = (Cq^\gamma/\Omega)^{1/2} \exp(i\mathbf{q}\mathbf{r})$, where \mathbf{q} is the phonon wave vector, Ω is the normalizing volume, and $\gamma = +1$ for deformation coupling and -1 for piezoelectric coupling. Interaction constants C for both types of interaction may be found, for example, in Refs. 1–5. The piezoelectric interaction, in fact, also depends on the direction of q but for simplici-

ty we follow the usual practice of taking an average over all directions.¹⁸ This does not change any qualitative results, particularly in the one-dimensional problem where the direction of electron momentum $\hbar\mathbf{k}$ is fixed relative to the crystal axes. There will, however, be a small change in the numerical factors in C for the different temperature intervals considered as already noted for the 3D (Ref. 19) and 2D (Ref. 5) cases.

By Fermi's golden rule, the probability of spontaneous emission of phonons with wave vector \mathbf{q} is given by

$$W(\mathbf{q}) = \frac{2\pi Cq^\gamma}{\hbar\Omega} \sum_{N,M} \sum_k |\langle N, k | \exp(i\mathbf{q}\mathbf{r}) | M, k - q_y \rangle|^2 \delta[\hbar\omega(N-M) + \hbar^2 k q_y / m - \hbar^2 q_y^2 / (2m) - \hbar s q] \\ \times f_e[\hbar\omega(N + \frac{1}{2}) + \hbar^2 k^2 / (2m)] \{ 1 - f_e[\hbar\omega(N + \frac{1}{2}) + \hbar^2 k^2 / (2m) - \hbar s q] \}, \quad (3)$$

where s is the sound velocity. Similar expressions can be obtained for absorption and stimulated emission and by combining these it can readily be shown that the net energy-loss rate per electron is given by

$$Q = (\nu L_y)^{-1} \sum_q \hbar s q W(\mathbf{q}) \\ \times \frac{1 - \exp[\hbar s q (1/k_B T_e - 1/k_B T)]}{1 - \exp(-\hbar s q / k_B T)}, \quad (4)$$

where L_y is the sample length along the y axis.

From Eq. (3) it can be seen that the frequency and angular distributions of the phonons emitted from the 1DEG are determined by a series of energy and momentum constraints. The product $f_e(1-f_e)$ ensures that the phonon energy cannot exceed the width of the Fermi distribution:

$$\hbar s q \lesssim k_B T_e \quad (5)$$

and, for a transition between the N th and M th electronic subbands, the combination of energy and y -component momentum conservation requires that q_y is given by

$$k q_y - q_y^2 / 2 + m \omega(N-M) / \hbar - m s q / \hbar = 0, \quad (6)$$

where $k \sim k_N = \sqrt{2m[E_F - \hbar\omega(N + cf12)]} / \hbar$, the Fermi wave vector in the N th subband. Since the electrons are confined in the x and z directions, exact momentum conservation in these directions is replaced by the inequalities

$$q_x \lesssim \pi / l, \quad (7a)$$

$$q_z \lesssim \pi / a, \quad (7b)$$

where a is the characteristic thickness of the 2DEG. We mainly restrict the present analysis to temperatures for which $a \lesssim \pi \hbar s / k_B T_e$. For this range the restriction set by (5) is always more severe than of (7b) with the result that the characteristic value of q_z is determined by

$$q_z \lesssim k_B T_e / \hbar s \quad (8)$$

and the matrix element of $\exp(iq_z z)$ is always equal to

unity.

The condition $a \lesssim \pi \hbar s / k_B T_e$ for $a \simeq 5$ nm corresponds to temperatures less than 45 and 25 K for quantum wells in Si and GaAs, respectively, although this becomes more restrictive in single heterostructures (and metal-oxide-semiconductor field-effect transistors) because of the difference in the wave functions. Optical-phonon emission is negligible in this temperature range (e.g., Ref. 20).

As a rule, the lateral confinement in a 1DEG is not as strong as the confinement along the z axis. Therefore, the most severe restriction on q_x may be either (5) or (7a) depending on the relative sizes of $k_B T_e$ and $\hbar s l^{-1} = (m s^2 \hbar \omega)^{1/2}$. It is convenient to give separate consideration to the different temperature ranges.

III. RANGE (i) $k_B T_e \ll (m s^2 \hbar \omega)^{1/2}$

In this case restriction (5) is more severe than (7a). Hence q_x as well as q_z is typically of order $k_B T_e / \hbar s$ and the total matrix element in (3) is δ_{NM} which means that interlevel (intersubband) processes are absent. The component q_y is given by Eq. (6) with $M=N$. Since $k_N \gtrsim l^{-1} \gg k_B T_e / \hbar s \gtrsim q$, we can neglect the term of order q_y^2 to obtain

$$|q_y| \sim m k_B T_e / \hbar^2 k_N \ll |q_x|, |q_z|. \quad (9)$$

So the phonons are emitted almost normal to the axis of the 1DEG and isotropically in the xz plane (the intensity distribution will not, in general, be isotropic because of phonon focusing in the substrate). From (6) it can be seen that the peak of the emission, in fact, occurs at a small angle θ_N normal to the 1DEG axis where $(\pi/2 - \theta_N)$ is the Čerenkov angle $\cos^{-1}(m s / \hbar k_N)$ and evidently depends on the subband responsible for the emission.

The expression for $W(\mathbf{q})$ can now be integrated over k to obtain

$$W(\mathbf{q}) = \frac{2Cq^\gamma mL_y}{\hbar^3 \Omega |q_y|} \sum_N \left[\exp \left[\frac{ms^2 q^2}{2k_B T_e q_y^2} - \frac{E_F - \hbar\omega(N + \frac{1}{2})}{k_B T_e} \right] + 1 \right]^{-1} \times \left[\exp \left[-\frac{ms^2 q^2}{2k_B T_e q_y^2} + \frac{\hbar s q + E_F - \hbar\omega(N + \frac{1}{2})}{k_B T_e} \right] + 1 \right]^{-1}. \quad (10)$$

It is interesting to compare (10) with the analogous phonon distribution for a 2DEG in the case when the wave-vector component in the xy plane q_{\parallel} is less than $msq/\hbar k_N$. In this system electrons also emit phonons isotropically in the plane normal to the electron momentum k . But this can now have any direction in the xy plane, so in this range the 2DEG emission is the same as that from a set of 1DEG's randomly oriented in the plane and by averaging (10) we obtain

$$W(\mathbf{q}) \cong \frac{2Cq^{\gamma+1} m^2 s}{\pi \hbar^4 L_z k_F q_{\parallel}} \left[\exp \left[\frac{\hbar s q}{k_B T_e} \right] - 1 \right]^{-1}. \quad (11)$$

Since $W(\mathbf{q}) \propto 1/q_{\parallel}$, the emission is strongest normal to the plane: this is the only direction in which the total intensity is the sum of the intensities from each of the 1DEG's. So the statement in Refs. 2 and 5 that the emission from a 2DEG becomes isotropic at low temperatures is not exact.

Returning to the one-dimensional problem we calculate the energy-loss rate Q per electron using (4) and (10). After somewhat cumbersome calculations we obtain

$$Q = \frac{Cmk_B^{\gamma+4}}{2\pi^2 \hbar^{\gamma+5} s^{\gamma+2} \nu} \Gamma(\gamma+4) \zeta(\gamma+4) [T_e^{\gamma+4} - T^{\gamma+4}] \times \sum_N \frac{1}{E_F - \hbar\omega(N + \frac{1}{2})}. \quad (12)$$

with a frequency distribution

$$Q(\omega_p) \propto \frac{\omega_p^{\gamma+3}}{\exp(\hbar\omega_p/k_B T_e) - 1} \quad (\text{for } T_e \gg T),$$

where $\omega_p = sq$ is the phonon frequency. It can be seen that Q oscillates with the electron density ν having peaks when $E_F(\nu)$ coincides with the density of states singularity near the bottom of a one-dimensional subband (the possibility of these oscillations was also pointed out in Ref. 12). In real structures, the singularities are smoothed by carrier scattering. If we assume Lorentzian broadening corresponding to a scattering time τ , $1/\varepsilon$ in (12) [$\varepsilon = E_F - \hbar\omega(N + \frac{1}{2})$] is replaced by

$$\frac{\tau}{2(\varepsilon^2 \tau^2 + 1)(\sqrt{\varepsilon^2 \tau^2 + 1} - \varepsilon \tau)}.$$

If many subbands are occupied, as is the case in most

real structures, then away from the peaks, the sum in (12) can be replaced by an integral of value $(1/3\hbar\omega) \ln(9\pi^2 \hbar \nu^2 / 32m\omega)$, where we have used the expression for E_F given by Eq. (2b). For this case the value for Q essentially only differs from the corresponding expression for a two-dimensional system² by the logarithmic factor in spite of the marked difference in the angular distributions. The similarity of the two- and three-dimensional expressions has already been emphasized in Ref. 2 and it can now be seen that this also extends to one-dimensional systems. This statement is also confirmed by numerical calculations.¹²

IV. RANGE (ii) ($ms^2 \hbar\omega)^{1/2} \ll k_B T_e \ll \hbar\omega, E_F$)

The nature of the phonon emission differs from that in range (i) in two important respects. The first is that phonons can now be emitted from intersubband as well as intrasubband transitions, and the second is that since $k_B T_e / \hbar s \gg l^{-1}$, the characteristic value of q_x is determined by l^{-1} rather than T_e . This second change will be shown to modify the angular dependence of the emission and reduce the power-law dependence of Q on T_e .

There are now three possible kinds of electron transitions as shown in Fig. 1. There are intrasubband small-angle transitions with $|q_y| \approx msq/\hbar k$, as in (i) (labeled 1 in Fig. 1), intrasubband backscattering transitions with $|q_y| \approx 2k_N$, and intersubband scattering transitions with $|q_y| \approx |k_N \pm k_M|$ (labeled, respectively, 2 and 3). In process 1, $q_y \ll q_x$ whereas in the two latter processes $q_y \sim q_x$. In all three cases $q_x, q_y \ll q_z$ so that the phonons are emitted essentially normal to the plane of the original 2DEG. The distribution function now consists of two components:

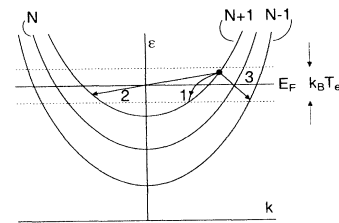


FIG. 1. Schematic picture of the different types of electron-phonon processes allowed in temperature range (ii). The dashed lines indicate the approximate extent of the thermal smearing of the Fermi distribution.

$$\begin{aligned}
W(\mathbf{q}) = & \frac{2Cq^\gamma mL_y}{\hbar^3 \Omega} \left\{ \sum_N Q_{NN}^2(q_x^2 l^2 / 2) \frac{1}{|q_y|} \left[\exp \left[\frac{ms^2 q^2}{2q_y^2 k_B T_e} - \frac{E_F - \hbar\omega(N + \frac{1}{2})}{k_B T_e} \right] + 1 \right]^{-1} \right. \\
& \times \left[\exp \left[-\frac{ms^2 q^2}{2q_y^2 k_B T_e} + \frac{\hbar sq + E_F - \hbar\omega(N + \frac{1}{2})}{k_B T_e} \right] + 1 \right]^{-1} \\
& + \sum_{N, M, \pm} \frac{Q_{MN}^2(q_x^2 l^2 / 2)}{|k_N \pm k_M|} \left[\exp \left[\frac{\hbar^2 k_N k_M}{mk_B T_e |k_N \pm k_M|} (q_y \pm k_N \pm k_M) \right] + 1 \right]^{-1} \\
& \left. \times \left[\exp \left[-\frac{\hbar^2 k_N k_M}{mk_B T_e |k_N \pm k_M|} (q_y \pm k_N \pm k_M) + \frac{\hbar sq}{k_B T_e} \right] + 1 \right]^{-1} \right\} \equiv W_1(\mathbf{q}) + W_2(\mathbf{q}), \quad (13)
\end{aligned}$$

where $W_2(\mathbf{q})$ includes processes 2 and 3 and $Q_{MN}(t) = (M!/N!)^{1/2} \exp(-t/2) t^{(N-M)/2} L_M^{N-M}(t)$ are the matrix elements of $\exp(iq_x x)$ [$L_\alpha^\beta(t)$ are associated Laguerre polynomials, $M \leq N$].

In spite of the very different phonon frequencies generated in intrasubband and intersubband transitions, these two types of transitions [two terms in (13)] give approximately equal contributions to Q so that the net energy-loss rate per electron can be written as a single formula:

$$Q = \frac{Cmk_B^{\gamma+3}}{\pi^3 l \hbar^{\gamma+4} s^{\gamma+1} \nu} \Gamma(\gamma+3) \zeta(\gamma+3) [T_e^{\gamma+3} - T^{\gamma+3}] \sum_{M, N} \frac{\lambda_{MN}}{[E_F - \hbar\omega(M + 1/2)]^{1/2}} \frac{1}{[E_F - \hbar\omega(N + 1/2)]^{1/2}}, \quad (14)$$

where

$$\lambda_{MN} = l \int_{-\infty}^{\infty} Q_{MN}^2(q_x^2 l^2 / 2) dq_x = \frac{1}{s^{M+N-1} M! N!} \int_{-\infty}^{\infty} \exp(-2x^2) H_M^2(x) H_N^2(x) dx$$

(H_N is the Hermite polynomial) and now

$$Q(\omega_p) \propto \frac{\omega_p^{\gamma+2}}{\exp(\hbar\omega_p / k_B T_e) - 1} \quad (T_e \gg T).$$

It can be seen that, as in range (i), Q oscillates with ν with peaks when E_F coincides with the bottom of a subband but its temperature dependence is less in power by 1 than in range (i) [Eq. (12)]. This results from the fact that q_x is now limited by l^{-1} so that its contribution to the phase volume is independent of T_e while in range (i) it increases linearly with T_e .

V. RANGE (iii) $kT_e \sim \hbar\omega$

One additional type of electron-phonon process becomes possible in this temperature range. It results from electron transitions between peaks in the one-dimensional density of states at $E = \hbar\omega(N + \frac{1}{2})$ and gives rise to the emission of "resonant" phonons of energy $j\hbar\omega$ where j is an integer. It leads to additional terms ΔW and ΔQ in W and Q where

$$\begin{aligned}
\Delta W \simeq & \frac{2Cq^\gamma mL_y}{\hbar^3 \Omega |q_y|} \sum_{M, N} Q_{MN}^2(q_x^2 l^2 / 2) \left[\exp \left[\frac{\hbar\omega(N + \frac{1}{2}) - E_F}{k_B T_e} + \frac{m[sq - \omega(N - M)]^2}{2k_B T_e q_y^2} \right] + 1 \right]^{-1} \\
& \times \left[\exp \left[\frac{E_F - \hbar\omega(N + \frac{1}{2})}{k_B T_e} - \frac{m[sq - \omega(N - M)]^2}{2k_B T_e q_y^2} + \frac{\hbar sq}{k_B T_e} \right] + 1 \right]^{-1}. \quad (15)
\end{aligned}$$

Since $q \simeq (\omega/s)j \gg |q_x|, |q_y| \sim l^{-1}$, phonons are largely emitted normal to the 2DEG plane. The total emission rate $\Delta Q \lesssim Q$ and the intensities of the quasimonochromatic peaks at ωj in the phonon frequency spectrum fall off as $\exp(-\hbar\omega j / k_B T_e)$. It is interesting that they do not depend on the position of the Fermi level in contrast to the processes discussed earlier and shown in Fig. 1. This is readily seen when $k_B T_e \ll \hbar\omega$. Let $E_F = \hbar\omega(N + \frac{1}{2}) + \delta$ ($\delta < \hbar\omega$). Since the electron concentration at the bottom of the $(N+1)$ th subband $\sim \exp[-(\hbar\omega - \delta) / k_B T_e]$ and the concentration of holes

(unoccupied states) at the bottom of the N th subband $\sim \exp(-\delta / k_B T_e)$, their product, which determines the transition probability, is independent of δ . To confirm this more generally, we have calculated the additional energy-loss rate ΔQ arising from (15) and found that it is, indeed, independent of E_F . Its value is given by an expression similar to (14) and with the same temperature dependence but with the factor responsible for the oscillations $1/[E_F - \hbar\omega(M + \frac{1}{2})]^{1/2} [E_F - \hbar\omega(N + \frac{1}{2})]^{1/2}$ replaced by $1/\hbar\omega$. In fact, the oscillations in (14) also become very heavily damped in this temperature range

since their amplitude is proportional to a term $\chi/sh(\chi)$ ($\chi=2\pi^2k_B T_e/\hbar\omega$) similar to that responsible for the damping of the Shubnikov–de Haas oscillations in resistivity.

VI. MAGNETIC-FIELD DEPENDENCE OF THE PHONON EMISSION

We next consider the effect of magnetic field on the energy relaxation in a 1DEG. It is well known (see, e.g., Ref. 21) that if a parabolic confining potential is used to form the 1DEG and a magnetic field is applied normal to the 2DEG plane, the resulting Schrödinger equation can be solved exactly. The energies, in fact, remain the same as those of (1b) but with the oscillator frequency ω and the effective mass m replaced by the field-dependent quantities

$$\tilde{\omega} = \sqrt{\omega^2 + \omega_c^2} \quad \text{and} \quad \tilde{m} = m \frac{\tilde{\omega}^2}{\omega^2} \quad \left[\omega_c = \frac{eB}{m} \right]. \quad (16)$$

The wave functions $\langle N, k |$ remain harmonic oscillator functions but with frequency $\tilde{\omega}$, center coordinate $x_0 = (k\hbar/eB)(\omega_c/\tilde{\omega})^2$, and the confinement length reduced from l to $(\hbar/m\tilde{\omega})^{1/2}$. It can be seen that the effect of a magnetic field on a 1DEG is only significant when B is such that $\omega_c \gtrsim \omega$. The discussion is restricted to this case.

The presence of a magnetic field modifies the previous analysis in two ways. The first is due to the changes in the energy spectrum and the second to the creation of a spatial separation of the $\langle k |$ and $\langle k - q_y |$ wave functions. This separation, which increases linearly with q_y , diminishes the overlap of the wave functions in the matrix element and provides a restriction on the maximal value of q_y . This arises through the matrix elements Q_{MN} which now become functions of the combination $[q_x^2 + q_y^2(\omega_c/\tilde{\omega})^2]^{1/2}$ rather than of q_x . In fact, except at very high fields, this restriction on q_y has only a modest effect on the total power emitted since nearly all the phonons in temperature range (i) and a sizable fraction ($\sim \frac{1}{2}$) in ranges (ii) and (iii) have rather small values of $q_y \sim mk_B T_e / \hbar k_N$. The effect should, however, be detectable through the suppression of the wings of the angular distribution of phonon emission in ranges (ii) and (iii).

One result of the changes in the energy spectrum is that since ω in formulas (12) and (14) now becomes the field-dependent frequency $\tilde{\omega}$, the energy-loss rate will oscillate with B as well as with E_F in a similar way to the conductivity of a 1DEG (see, e.g., Ref. 22).

Another effect of a magnetic field is the change in the characteristic temperature determining the boundary between ranges (i) and (ii) due to the increase in effective mass m (or decrease in confinement length). So an increase in field can transfer the system from range (ii) or (iii) to range (i) causing changes in the size and temperature dependence of Q and also changes in the angular dependence of the emission.

It is also worth noting that since ω and m are replaced by $\tilde{\omega}$ and \tilde{m} , the magnetic field also modifies the relation

between electron density ν and Fermi energy E_F to

$$\nu = \frac{2}{\pi\hbar} \sum_N \sqrt{2\tilde{m} [E_F - \hbar\tilde{\omega}(N + \frac{1}{2})]} \quad (17)$$

[for $B=0$ this expression in the limiting cases gives (2a) and (2b)]. Figure 2 illustrates the effect of this on $E_F(B)$ for two electron densities. Because E_F varies with field, the magnetic-field dependence of Q (as well as of some other electronic properties) measured for $\nu = \text{const}$ differs from that measured for $E_F = \text{const}$. In principle, both these situations can be realized experimentally.

We consider the $Q(B)$ dependence for low T_e corresponding at $B=0$ to range (i). At low fields it will be described by formula (12) which is proportional to m/ν . Therefore, the monotonic part of Q increases steadily with B , proportional to \tilde{m} if ν is held constant or proportional to $\tilde{m}^{1/2}$ if E_F is held constant. Eventually, however, $\tilde{m}s^2/2$ becomes greater than $E_F - \hbar\tilde{\omega}(N + \frac{1}{2})$ so that s exceeds the Fermi velocity in the subband. At this point, phonon emission from intrasubband transitions becomes impossible except from the exponentially small proportion of electrons of velocity $v > s$. Formally it means that we cannot neglect $q_y/2$ in the momentum conservation law (6). The calculations show that for $T=0$ each term in (12) must be multiplied by the factor

$$\frac{1}{\Gamma(\gamma+4)\zeta(\gamma+4)} \int_0^\infty \frac{x^{\gamma+2}}{e^x - 1} \ln \left[\frac{\phi + e^x}{\phi + 1} \right] dx, \quad (18)$$

where

$$\phi = \exp \left[\frac{\tilde{m}s^2/2 - E_F + \hbar\tilde{\omega}(N + \frac{1}{2})}{k_B T_e} \right].$$

It is seen that for $\phi > 1$ this factor is proportional to

$$\exp \left[\frac{E_F - \hbar\tilde{\omega}(N + \frac{1}{2}) - \tilde{m}s^2/2}{k_B T_e} \right]$$

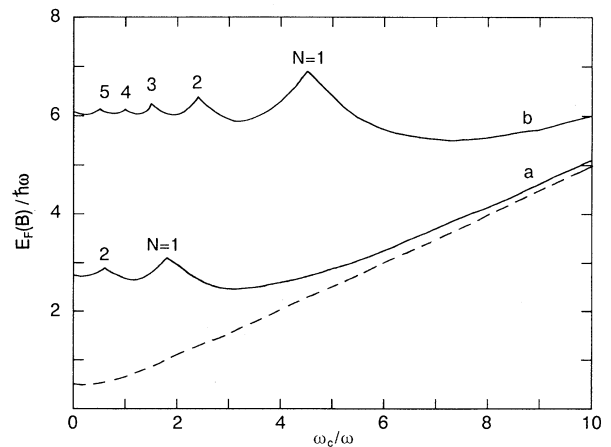


FIG. 2. Magnetic-field dependence of the Fermi energy in 1DEG for $\pi\nu(\hbar/8m\omega)^{1/2} = 3$ (curve a) and 10 (curve b). Peaks occur when E_F coincides with the bottom of the N th subband. The dashed line indicates the $N=0$ level position, $\hbar\tilde{\omega}/2$.

and, hence, decreases exponentially with B . For finite T we need to subtract from this expression a similar one with T_e replaced by T .

The rise in $Q(B)$ below the N th maximum is due to the increase in the density of electron states and the fall is caused initially by the rapid decrease in emission rate when the Fermi velocity v_F falls below the sound velocity [$E_F - \hbar\omega(N + \frac{1}{2}) < \tilde{m}s^2/2$]. This is followed soon after by depopulation of the N th subband when $E_F < \hbar\omega(N + \frac{1}{2})$. So as the field increases, $Q(B)$ goes through a sequence of oscillations at low fields ($\omega \lesssim \omega_c \ll E_F/\hbar$) until essentially all the electrons are in the $N=0$ subband. For $v=\text{const}$ the rise in $Q(B)$ that occurs is entirely due to the increase in \tilde{m} and the fall above a critical field B_c to $v_F < s$ since, of course, this level cannot be depopulated.

For $\omega_c \gg \omega$, the critical field is given by

$$B_c = \frac{\hbar\omega^2}{2es^2} \left[-1 + \left[1 + \frac{8ms^2E_F}{\hbar^2\omega^2} \right]^{1/2} \right] \quad (19a)$$

for a given E_F and by

$$B_c = \frac{\omega}{e} \left[\frac{\pi\hbar m v}{2s} \right]^{1/2} \quad (19b)$$

for a given v .

An example of the whole $Q(B)$ dependence is given in Fig. 3 for a 1DEG with $T_e=2$ K. We assume $v=\text{const}$ and also examine the effect of level broadening (see Sec. III). By comparing the two curves in the figure one can see that the electron scattering drastically reduces the oscillation amplitude but has much less influence on the high-field maximum of Q (note the change in the magnetic-field scale in Fig. 3 above $B=2$ T). The oscillations also decrease in amplitude with an increase in T_e .

The field-dependent changes in Q are accompanied by changes in the angular distribution of the emission. The Čerenkov angle $\cos^{-1}(s\tilde{m}/\hbar k_N)$ for the N th subband be-

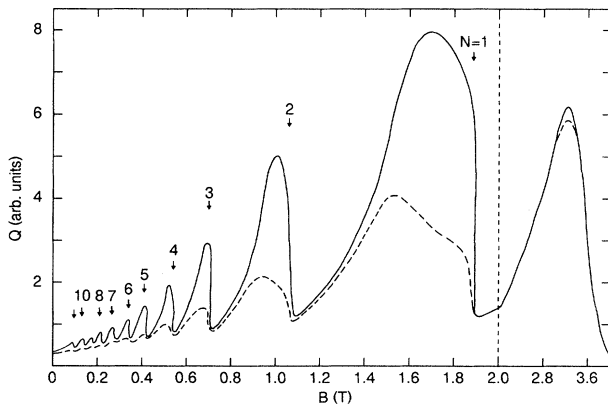


FIG. 3. Magnetic-field dependence of Q corresponds to $v=\text{const}$ for a GaAs 1DEG structure with $E_F(B=0) = 12.5\hbar\omega = 4$ meV, $T_e=2$ K. The collisional level broadening parameter $\omega\tau=3$ (solid line) and $\omega\tau=1$ (dashed line). The sharp falls in Q indicated by the arrows occur when the bottom of a 1D subband moves through the Fermi energy.

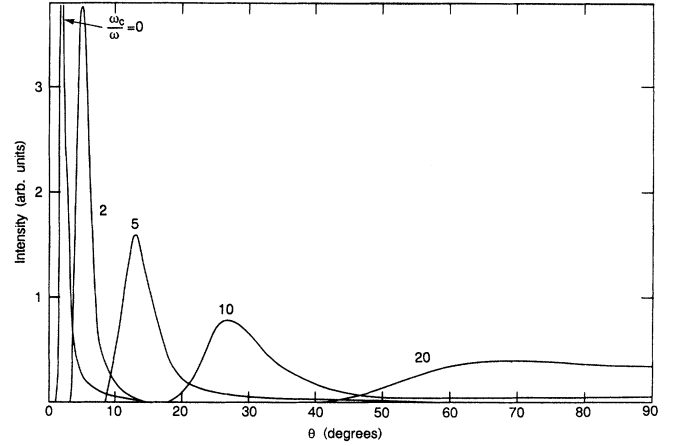


FIG. 4. Angular dependences of the emitted power for a GaAs structure with $T_e=5$ K, $E_F=2$ meV at different magnetic fields: $\omega_c/\omega=0, 2, 5, 10,$ and 20 . ϕ is the angle with the wire direction (y axis).

comes zero near the maxima of the oscillations so as the field increases, the emission becomes steadily more isotropic. This effect starts with the emission from the higher subbands and extends to the lower subbands with increasing field. To describe this effect quantitatively, it is convenient to introduce a function

$$W(\phi, \alpha) = \hbar s \int q^3 W(\mathbf{q}) d\mathbf{q} \quad (20)$$

representing the angular distribution of the total emitted power (here ϕ is the angle between \mathbf{q} and the axis of the 1DEG and α is the polar angle in the xz plane). Figure 4 demonstrates the evolution of this function in magnetic fields at fairly low temperatures where there is no α dependence. At higher temperatures, corresponding at $B=0$ to range (ii), this evolution is preceded by the disappearance of the α dependence as a result of the transition to range (i) with increasing field.

VII. CONCLUSION

In this paper we have considered, for a wide range of electron temperature T_e , the various processes of acoustic-phonon emission that can occur from a heated 1DEG. The angular distribution of the phonons changes considerably as the electron temperature is changed but there is less change in the expressions for the frequency spectrum $Q(\omega_p)$ and the total energy-loss rate per electron, $Q(T_e)$, and for temperatures greater than $(ms^2\hbar\omega)^{1/2}/k_B$ Eq. (14) should provide a good description up to $k_B T_e \sim \hbar s/a$. The reason for this is that q_x and q_z retain the same value or form over this range ($|q_x| \sim l^{-1}$, $|q_z| \sim k_B T_e/\hbar s$) as does the change $\Delta q_y \sim mk_B T_e/\hbar k_N$ from its mean value (0 or $k_N \pm k_M$) that occurs as T_e is increased. So the volume of phase space occupied by the wave vectors of the emitted phonons increases steadily with T_e over the entire range. The form of $Q(T_e)$ does change however when $k_B T_e > \hbar s/a$. For these temperatures q_z becomes limited

by a^{-1} rather than $k_B T_e$ resulting in a decrease in the temperature dependence of $Q(T_e)$ from $T_e^{\gamma+3} - T^{\gamma+3}$ to $T_e^{\gamma+2} - T^{\gamma+2}$. The frequency spectrum $Q(\omega_p)$ also retains the same form throughout range (ii) but at higher temperatures "monochromatic" lines appear at ω_j ($j=1,2,\dots$). At even higher temperatures there is a changeover from acoustic- to optic-phonon emission. A noticeable feature at low temperatures is the oscillatory behavior of $Q(T_e)$ when the Fermi energy is moved through the 1D energy-level spectrum.

Much more striking changes with T_e are seen in the angular dependence of the emitted phonons. At low temperatures [range (i)] the emission occurs equally in all directions close to the normal to the 1DEG axis. It is, in fact, peaked at a series of angles from the normal $\cos^{-1}(ms/\hbar k_N)$, though high resolution would be needed to resolve these peaks. As the temperature rises into range (ii), the isotropy in the xz plane (with intensity modified by phonon focusing) becomes broken and the emission is eventually restricted to directions close to the normal to the original 2DEG. The image of the emission on the opposite face from a short 1DEG sample would consist of an ellipse ($q_x \sim q_y$) from half the emission superimposed on a narrow strip ($q_y \ll q_x$) perpendicular to the 1DEG axis due to the other half. In the y direction the intensity falls to a minimum at the image center ($q_y=0$) but no similar effect occurs in the x direction. A further rise in temperature results in an additional circular component to the image due to the resonant phonons. This rich information contained in the angular distribution of the emission promises to give considerable detail on the electron-phonon interaction and similar conclusions should also apply to measurements of the ab-

sorption and transmission coefficients.

These various features of the phonon emission are all very sensitive to the application of quantizing magnetic fields perpendicular to the plane of the 2DEG. At low temperatures [range (i)] the energy loss, which is due to intrasubband transitions, first oscillates with magnetic field and then falls sharply above a critical field B_c as shown in Fig. 3. At higher temperatures the intersubband transitions including the contribution from the monochromatic phonons are also suppressed once $\bar{\omega}/s$ exceeds the inverse thickness of the 2DEG. The angular distribution becomes much more isotropic with increasing field. At low temperatures [range (i)] this results in the strip component of the image on the opposite face becoming steadily broader as $B \rightarrow B_c$ while at higher temperatures [range (ii)] the ellipse caused by intrasubband transitions becomes a narrow strip parallel to the 1DEG axis which becomes broader as the field moves the system towards range (i). Very similar effects should again be apparent in the phonon absorption, etc.

Finally we discuss briefly the neglect of screening in these calculations. In 2DEG's screening produces significant changes in both the magnitude and temperature dependence of Q .⁵ However in 1DEG's the screening is much weaker and has a logarithmic character²³ so the screening has little effect on $Q(T_e)$.

ACKNOWLEDGMENTS

We are very grateful to Dr. A. J. Kent, Dr. V. M. Rampton, and Dr. F. W. Sheard for discussions and the European Community for financial support.

- ¹P. J. Price, *J. Appl. Phys.* **53**, 6863 (1982).
²V. Karpus, *Fiz. Tekh. Poluprovodn.* **20**, 12 (1986) [*Sov. Phys. Semicond.* **20**, 6 (1986)].
³Y. H. Xie, R. People, J. C. Bean, and K. W. Wecht, *Appl. Phys. Lett.* **49**, 283 (1986).
⁴S. J. Manion and K. Hess, *J. Appl. Phys.* **62**, 4942 (1987).
⁵V. Karpus, *Fiz. Tekh. Poluprovodn.* **22**, 439 (1988) [*Sov. Phys. Semicond.* **22**, 268 (1988)].
⁶G. A. Toombs, F. W. Sheard, D. Neilson, and L. J. Challis, *Solid State Commun.* **64**, 557 (1987).
⁷K. A. Benedict, *J. Phys. Condens. Matter* **3**, 1279 (1991).
⁸W. Dietsche, in *Proceedings of the Third International Phonon Physics Conference, Heidelberg*, 1989, edited by S. Hunklinger et al. (World Scientific, Singapore, 1990), p. 767.
⁹L. J. Challis, A. J. Kent, and V. W. Rampton, *Semicond. Sci. Technol.* **5**, 1179 (1990).
¹⁰A. K. M. Wennberg, S. M. Ytterboe, C. M. Gould, H. M. Bozler, J. Klem, and H. Morkoç, *Phys. Rev. B* **34**, 4409 (1986).
¹¹A. M. Kreschuk, M. Yu. Martisov, T. A. Polyanska, I. G. Savel'ev, I. I. Saidashev, A. Ya. Shik, and Yu. V. Shmartsev, *Solid State Commun.* **65**, 1189 (1988).
¹²U. Bockelmann and G. Bastard, *Phys. Rev. B* **42**, 8947 (1990).
¹³L. J. Challis and A. Y. Shik, in *Phonon Scattering in Condensed Matter*, edited by M. Meissner and R. O. Pohl (Springer-Verlag, Berlin, in press).
¹⁴M. Buttiker, *Phys. Rev. B* **38**, 9375 (1988).
¹⁵A. Ya. Shik, *Fiz. Tekh. Poluprovodn.* **19**, 1488 (1985) [*Sov. Phys. Semicond.* **19**, 915 (1985)].
¹⁶S. E. Laux and F. Stern, *Appl. Phys. Lett.* **49**, 91 (1986).
¹⁷A. C. Warren, D. A. Antoniadis, and H. I. Smith, *IEEE Electron Devices Lett.* **EDL-7**, 413 (1986).
¹⁸V. F. Gantmakher and Y. B. Levinson, *Carrier Scattering in Metals and Semiconductors* (North-Holland, Amsterdam, 1987).
¹⁹J. D. Zook, *Phys. Rev.* **136**, A869, (1964).
²⁰P. Hawker, A. J. Kent, O. H. Hughes, and L. J. Challis, *Semicond. Sci. Technol.* **7**, B29 (1992).
²¹D. Childers and P. Pincus, *Phys. Rev.* **177**, 1036 (1969).
²²K. F. Berggren, T. J. Thornton, D. J. Newson, and M. Pepper, *Phys. Rev. Lett.* **57**, 1769 (1986).
²³S. G. Petrosyan and A. Ya. Shik, *Zh. Eksp. Teor. Fiz.* **96**, 2229 (1989) [*Sov. Phys. JETP* **69**, 1261 (1989)].